processes

MDPI

Article

Investigation on the Influence of Thermal Inertia on the Dynamic Characteristics of a Gas Turbine

Yang Liu, Yongbao Liu *, Yuhao Jia and Xiao Liang

College of Power Engineering, Naval University of Engineering, Wuhan 430033, China; ly136352168@163.com (Y.L.); slone77777@163.com (Y.J.); 13554688395@163.com (X.L.)
* Correspondence: liuyongbaoly@163.com

Abstract: In mini-grids and marine-isolated grids, power generation gas turbines are subjected to rapid start-up, shutdown, and acceleration/deceleration. This sudden load change can pose a significant impact on the power grid, severely affecting the operational characteristics of gas turbines. To understand the dynamic characteristics of the gas turbine in the transitional processes, this testing takes twin-shaft medium-sized power generation gas turbines as the test object, and goes through the process of startup, acceleration, deceleration, acceleration, shutdown in one hour, and repeats this process 40 times continuously. With fuel flow as the control parameter and power turbine outlet temperature and high-pressure turbine speed as the controlled parameters, the parameter response rate of the gas turbine under various transition processes is analyzed and the effect of thermal inertia on the gas turbine mass temperature as well as speed is studied. Research findings: During the transition processes, the gas temperature exhibited an axial gradient distribution in the channel. In both the acceleration and deceleration processes, the working fluid temperature gradually decreased along the flow direction. And thermal inertia posed different extents of impact on the dynamic characteristics of the gas turbine under different transitional processes. In the same transition process, the impacts of thermal inertia on the response speeds of temperature and rotational speed varied. The results of this study help to more accurately predict the operating state of the gas turbine during the transition process and lay the foundation for the dynamic simulation model of the non-adiabatic gas turbine.

Keywords: gas turbine; thermal inertia; dynamic characteristics; transition process; delayed responses

Citation: Liu, Y.; Liu, Y.; Jia, Y.; Liang, X. Investigation on the Influence of Thermal Inertia on the Dynamic Characteristics of a Gas Turbine. *Processes* **2024**, *12*, 1699. https://doi.org/10.3390/pr12081699

Academic Editor: Blaž Likozar

Received: 23 July 2024
Revised: 13 August 2024
Accepted: 13 August 2024
Published: 14 August 2024

1. Introduction

Gas turbines are characterized by high power, compact size, lightweight, rapid start-up, excellent acceleration performance, and high maneuverability, showcasing significant advantages in the power industry. Compared to traditional coal-fired power generation, modern gas turbines exhibit higher thermal efficiency. They can convert fuel energy into electricity more effectively, reducing energy waste. This efficient energy conversion makes gas turbines particularly important in supporting stable operation of the power grid and addressing peak power demands, thereby enhancing the operational efficiency and power generation quality of the power grid [1].

Rapid start-up, shutdown, and acceleration/deceleration are the primary modes of operation for modern gas turbines. In land-based microgrids and marine-isolated power grids, Load changes affect the grid and gas turbine operating conditions. A change in load requires the gas turbine to accelerate/decelerate to match the power demanded by the new load. So, the output power of the power system is determined by the load in land-based microgrids and marine-isolated power grids. The startup and shutdown of high-power equipment and sudden load fluctuations can cause instantaneous load changes. This sudden load change can pose a significant impact on the power grid, severely affecting the operational characteristics of gas turbines [2]. Hence, understanding the dynamic

characteristics of gas turbines under this transition process is crucial for the successful operation and maintenance of the power grid.

The dynamic characteristics of a gas turbine refer to the response and variation trend of the gas turbine during the variation in its operational state. In this paper, the dynamic characteristics of a gas turbine mainly refer to the gas turbine's response speed, i.e., the speed at which a gas turbine transitions from one stable state to another (e.g., how fast the gas turbine can reach a new stable operational state when the load or power demand changes).

During the stable operation of a gas turbine, a metal component and the gas in the channel, as well as different metal components, are in a state of thermal equilibrium. So, the influence of heat transfer on the characteristics of the gas turbine is small and can even be neglected [3]. During transitional processes, the axial temperature distribution of gas in the channel often responds rapidly to changes in the gas temperature at the combustor outlet. Due to thermal inertia effects caused by heat capacity, metal components originally in thermal equilibrium with the gas in the channel respond to temperature change more slowly than the gas. This characteristic results in a noticeable temperature difference between the gas and the metal components during the transition processes. This temperature difference causes substantial heat transfer between a metal component and the gas in the channel. Furthermore, this heat transfer leads to changes in the temperature of gas in the channel and aerodynamic parameters, ultimately causing variations in the actual operational characteristics of the gas turbine [4].

The influence of thermal inertia on the dynamic characteristics of a gas turbine mainly manifests as delayed responses in such operating parameters as the pressure loss and temperature of the gas, as well as the rotational speed [5]. With the advancement of modern gas turbine technology, the overall power and efficiency of gas turbines have gradually improved, along with an increase in the gas temperature within the channel during operation. As a result, larger temperature differences exist between the gas and metal components inside the gas turbine, as well as between the gas turbine and its external environment. Consequently, the impact of thermal inertia on the dynamic characteristics of gas turbines becomes increasingly remarkable [6,7].

Chapman et al. established a 1-D FEM model to predict the thermal displacement of the turbine shroud (along the radius direction) and rotor (along the thickness direction) [8,9]. By incorporating specific inertial modules to represent thermal inertia in an adiabatic one-dimensional gas turbine model, Wu et al. compared different simulation results and found that the acceleration/deceleration transitions of gas turbines considering the heat transfer effect are slower than those taking no account for the heat transfer effect. In the case of accelerated processes, for example, the average hysteresis rate is about 8% to 15%. The calculated results considering the heat transfer effect are more accurate than those regardless of the impact of the heat transfer effect [10,11].

The finite element method (FEM) was introduced by Chapman et al. to estimate the heat transfer rate between the high-pressure turbine, as well as the hub, and the working fluid [8]. Compared to the one-dimensional model, the finite element method provides a more detailed representation of the internal temperature distribution and can be applied more easily to components that consist of two materials.

Progress had been made by creating a heat transfer model that combined both the one-dimensional model and FEM by Chen et al. In this new model, the internal nodes in FEM had been replaced with lumped engine components, such as a lumped compressor stage or a lumped combustor. This allowed for the consideration of all engine components with proper settings. Additionally, the new internal nodes could account for heat conduction and radiation. The results show that the effect of heat transfer on the performance of the whole machine is mainly reflected by the response delay of each component. And the heat transfer effect has a significant impact on compressor performance [12].

Roclawski et al. investigated the transient performance of a radial turbine during load step operation conditions. The turbine CFD model was integrated into the transient loop, where the CFD model would directly estimate the turbine power instead of using

conservation equations [13]. By setting the temperature difference between the fluid and the wall, the transient performance of the turbine can be analyzed by steady state modeling.

Visser et al. studied the heat transfer effects of different components using a simplified heat transfer model for a two-shaft gas turbine under the same acceleration process and fueling plan. At the beginning of acceleration, the temperature of the low-pressure compressor was the lowest, and its heat transfer coefficient was also the lowest, hence its lowest heat flux density. Owing to excessive fuel, the heat transfer effect inside the combustor was most pronounced. After 3 s, as the temperature of gas passing through the turbine rose rapidly, the heat flux density on turbine components also increased rapidly, showing a heat transfer effect surpassing that in the combustor [14,15]. During most of the operating time of the gas turbine, the turbine components underwent the fiercest heat transfer effect.

In a transition process of a gas turbine, the gas in the channel of the compressor may experience a temperature increase due to the work done on it by the compressor blades. Yet, due to thermal inertia, the temperature change on the metal wall lags behind that of gas in the channel, leading to temperature differences that drive heat transfer effects. This result further affects the stability of the compressor. When considering thermal inertia, the surge boundary is reduced by 8% compared to an adiabatic model. However, the thermal inertia within the compressor components poses no significant impacts on other parameters of the compressor such as rotational speed, outlet temperature, and pressure ratio [16].

The combustor does not perform mechanical work by gas expansion since it primarily serves as the site for combustion reactions and does not have any rotating components. Hence, there is no need to consider the heat transfer effects driven by temperature differences between the combustor and metal wall, and thermal inertia has a minor impact on the combustor.

For turbines, there is also thermal inertia where the component temperature change lags behind the gas temperature change in the channel [17]. The gas inside the turbine reaches a higher temperature compared to the compressor, causing more pronounced heat transfer effects driven by the temperature difference with that on the metal wall. After undergoing the combustion and mixing process inside the combustor, the gas possesses uneven temperature and flow fields when passing the outlet of the combustor. This increases the convective heat transfer coefficient on the turbine blade surfaces, altering the aerothermal characteristics of the turbine. The resulting heat-driven secondary flow further reduces the efficiency of turbine stages [18]. Therefore, the dynamic characteristics of turbines in a gas turbine are affected by thermal inertia the most.

Although many scholars have studied the thermal inertia of gas turbines, most of them used the aerodynamic simulation method to investigate such issues as stability decrease and pressure loss of gas turbines caused by thermal inertia. With this method, they can obtain the conclusion that thermal inertia elongates the overall dynamic process time and causes derivation in the gas turbine's performance curves. However, it is difficult to make clear the specific influence of thermal inertia on the response time of a specific parameter (e.g., gas temperature and rotational speed) of the gas turbine. Yet, few studies were conducted by testing to probe into the response speed of a gas turbine under different transitional conditions. In this study, we tested a two-shaft gas turbine and analyzed its test data under different transitional processes (e.g., startup, acceleration, and deceleration). Based on this, we investigated the influence of thermal inertia on the responses of gas temperature and rotational speed in the gas turbine and discussed the reason why thermal inertia caused the lagged responses in the rotational speed and temperature under the transition process.

These data on temperature and speed response times of the gas turbine obtained in this test during different transitional processes can complement previous research on thermal inertia in terms of time scale. By combining this experimental data with previous aerodynamic simulation models, we can determine the specific trends and durations of temperature and speed changes during the gas turbine's transition process. This is significantly helpful for studying the reasons behind the lag in speed and temperature

responses due to thermal inertia during transition conditions and for more accurately predicting the gas turbine's operating state.

2. Test Scheme and Equipment

2.1. Selection of Test Parameters

In this test, the required test parameters include the flow rate of fuel, the rotational speed of the high-pressure turbine, and the outlet temperature of the power turbine.

During the operation of a gas turbine, the temperature of the high-speed gas in the channel often responds rapidly to changes in the flow rate of fuel. However, as a metal wall temperature response speed is notably slower than that of the gas in the channel due to thermal inertia. Consequently, a substantial temperature difference exists between the gas in the channel and the metal wall, thereby generating a heat transfer effect causing changes in the gas temperature [19]. Meanwhile, this process results in a lag in the temperature variation of the gas at the outlet of the channel. In this test, a segment of the channel in the acceleration process was taken as an example (Figure 1).

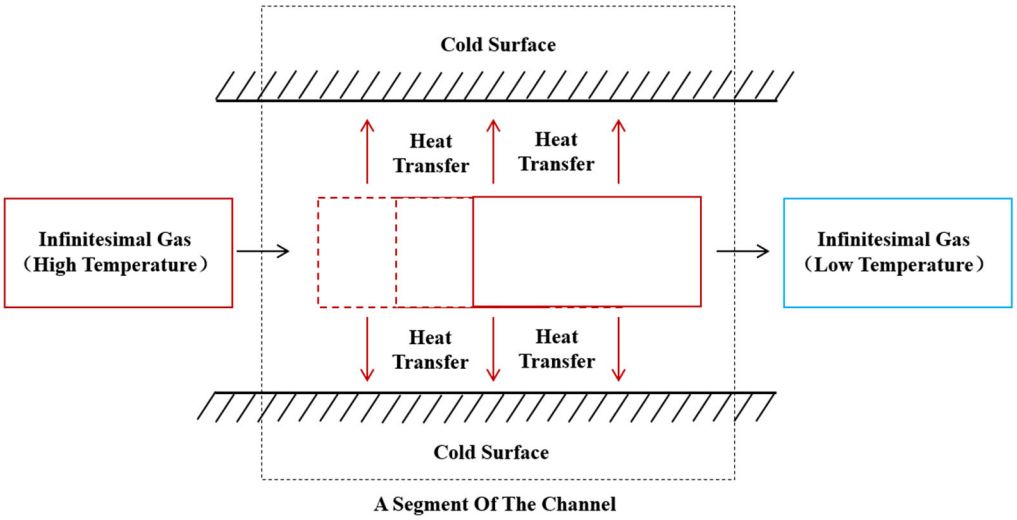

Figure 1. Heat transfer effects between gas flow and channel wall during acceleration.

The gas was treated as consisting of numerous infinitesimal elements, called the infinitesimal gas. When the gas turbine accelerated, the thermal equilibrium between the gas and the metal wall was disrupted, and the temperature of the gas began to exceed that of the metal wall. In a segment of the channel, the high-temperature infinitesimal gas transferred partial heat to the low-temperature wall through a heat transfer effect driven by the temperature difference between the fluid and the wall. This phenomenon persisted till a thermal equilibrium was reached between the wall and the gas. This heat transfer effect driven by the temperature difference would accumulate in each segment of the channel. On a macroscopic level, it manifested as axial gradient changes in the gas temperature within the entire channel and lagged temperature responses of the high-speed gas. Thus, the temperature response lag time of the gas at the outlet of the channel was used as an indicator by which thermal inertia affects the dynamic characteristics of the gas turbine.

In transitional processes, the heat transfer effect between the gas in the channel and the metal wall inevitably results in a change in the total enthalpy of the gas. When releasing heat to the metal wall, the gas experiences a loss in total enthalpy during the flow process, which ultimately leads to a reduction in its mechanical work capability [20]. When absorbing heat from the wall, the gas's total enthalpy increases, thereby enlarging its mechanical work capability. This fluctuation in the mechanical work capability affects, on the one hand, the gas's ability to overcome rotor inertia, and on the other hand, its ability to perform mechanical work on the gas turbine. This makes the rotational speed difficult to fully reach

the design value in a short time [21]. Therefore, when testing the influence of thermal inertia on the dynamic characteristics of the gas turbine, we also treated the response lag time and steady-state value of the rotational speed of the high-pressure turbine as indicators by which thermal inertia affects the dynamic characteristics of the gas turbine.

In the turbines, the gas performs mechanical work through expansion, and its energy is primarily reflected in its pressure and temperature. Changes in total temperature reflect variations in the total enthalpy of the gas, while changes in total pressure reflect variations in the flow rate of the gas.

The changes in both total temperature and total pressure of the turbines are synchronous since they are directly caused by the expansion and mechanical work of the gas. The loss of mechanical work capability of the gas caused by heat transfer effects is also reflected in the changes in rotational speed during the process where the gas drives the turbine. Based on the difference between the rotational speed of the high-pressure turbine after reaching a steady state and the design rotational speed of the gas turbine under this operating condition, we can obtain the loss of mechanical work capability of the gas caused by thermal inertia. Thereby, the influence of thermal inertia on the gas turbine can be accurately reflected just by measuring the changes in the total temperature of the gas and the rotational speed of the high-pressure turbine.

2.2. Design of the Test Scheme

To understand the variations in the response speeds of controlled parameters of the gas turbine under different transitional processes, common transitional conditions such as cold start, hot start, acceleration, and deceleration were integrated into a single test. This test was designed with a single-cycle control scheme as illustrated in Figure 2. The rated load was set at 1, with a cycle T of one hour. In one cycle, the gas turbine underwent the idling rating, accelerated start, deceleration, acceleration, and shutdown stages in turn. Under identical change extents in the load, the acceleration of a gas turbine generally takes a longer time than its deceleration. Hence, the acceleration time was designed 120 s longer than the deceleration time. Furthermore, a steady-state operation stage of 250 s was set between two dynamic change stages, allowing for the gas turbine to stabilize sufficiently after each dynamic change stage without interfering with the next stage. The gas turbine was set to operate through the stages in sequence within a single cycle by load increase/decrease. Considering the actual continuous operation time of the gas turbine and in order to exclude the influence of chance factors, the duration of the test is as long as possible. However, due to the test conditions and financial constraints, we finally chose a duration of 40 h.

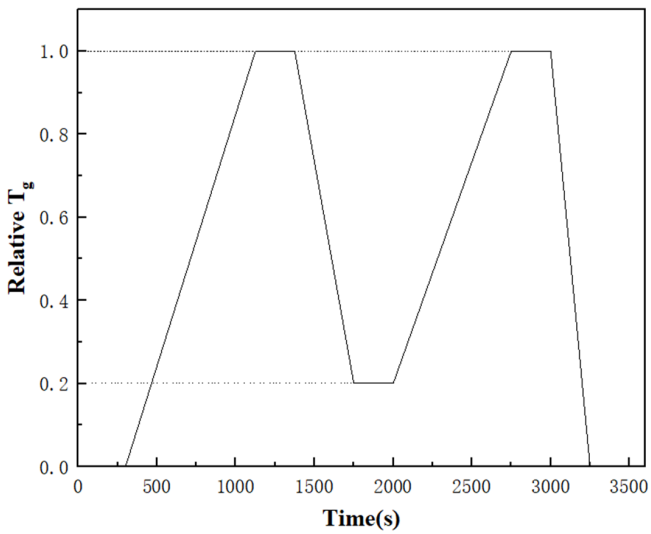

Figure 2. The single-cycle control scheme of the gas turbine.

The thermal inertia investigated in this study primarily occurred during the dynamic process of the gas turbine. Therefore, in this test, only the transitional stages between two steady-state operating conditions were analyzed. Besides, in the final stage (i.e., shutdown) of an operating cycle, the load dropped to zero. At the beginning of this stage, the fuel control system reduced the fuel flow to below 0.1 L/s quickly, maintaining an idle condition throughout this stage, and finally, the fuel control valve was closed. For most of the time during this stage, the control parameter G_f did not change significantly, making it impossible to calculate the parameter lag time. Therefore, this stage is not discussed here.

2.3. Preparation for Test Equipment

The test was conducted on the test bench of a specific model of a gas turbine generator set. Test data were collected using the temperature sensors installed on the gas turbine and the built-in rotational speed and fuel flow rate monitoring systems on the test bench.

The test bench mainly consists of a two-shaft megawatt gas turbine, an excitation rectifier generator, measurement and control equipment, and a control console (Figure 3). It can perform the following functions: start-up, acceleration, deceleration, full-load operation, normal shutdown, and emergency shutdown. The generator set can implement several load variation modes: load increase, load decrease, sudden load increase, sudden load decrease, and load shedding. The gas turbine section primarily includes the air intake cover, axial-flow compressor, annular combustor, axial-flow turbine, power turbine, exhaust housing, and casing (Figure 4). The gas turbine tested was a medium-sized, twin-shaft gas turbine designed to generate power for land-based microgrids and ocean-isolated grids. It is less than 10 MW and has an efficiency greater than 31%. It is about 7 m long and 3.7 m wide, not counting the outer protective box.

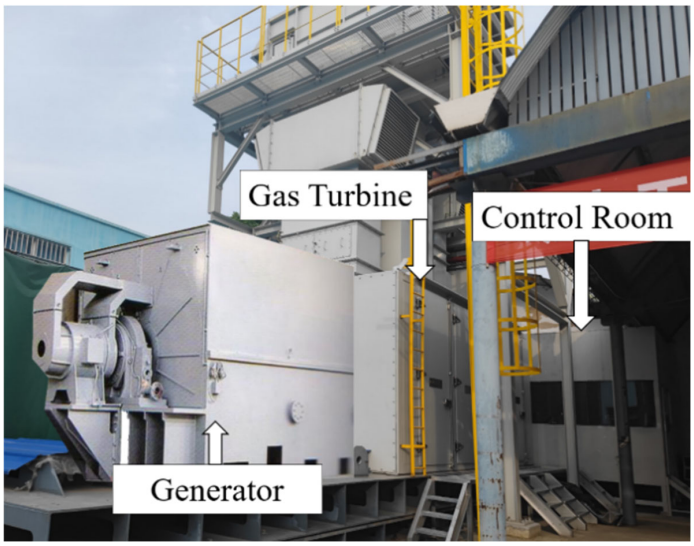

Figure 3. The test bench of a specific model of gas turbine generator set.

The rotational speed of the high-pressure turbine and the flow rate of fuel were recorded in real time by the built-in monitoring systems on the test bench. The gas temperature was measured by three temperature sensors installed at the power turbine outlet. KAIPUSEN brand WRNK-191 armored K-type thermocouples and associated signal transmission and receiving equipment (Figure 5) were adopted, with temperature measurements ranging from −50 °C to 1150 °C and a sampling frequency of 4 Hz. Three measurement sections z1~z3 were divided equally by the length of the barrel-shaped casing connecting the power turbine and the generator. Within each measurement section, four temperature sensors r1~r4 were uniformly and circumferentially arranged on the inner surface of the casing. Based on this arrangement, the 12 temperature sensors were positioned, as shown in Figure 6. To minimize the impact of non-uniform temperature

fields on the sections of the channel caused by cooling and mixing, the gas temperature on each section was valued by averaging the temperatures measured by the four temperature sensors arranged circumferentially on the section. The axially arranged temperature sensors allow for assessing axial temperature variations in the channel, thereby validating the conclusion regarding axial gradient changes in the gas temperature.

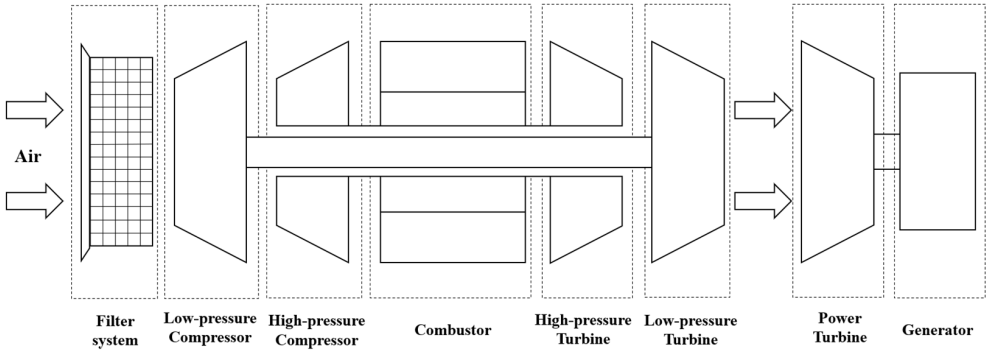

Figure 4. Diagram of a dual-shaft gas turbine structure.

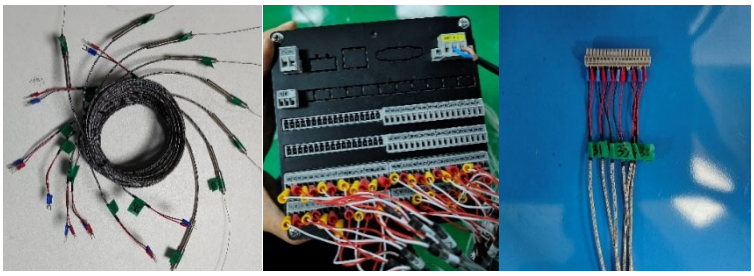

Figure 5. KAIPUSEN brand WRNK-191 armored K-type thermocouples and associated signal transmission and receiving equipment.

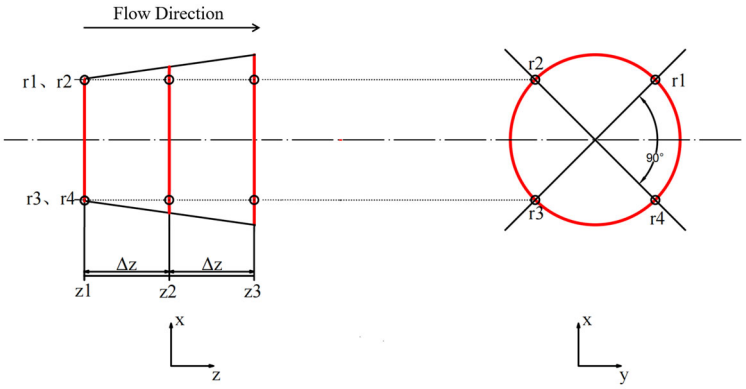

Figure 6. Distribution of temperature sensor locations.

3. Test Data Analysis Methods

3.1. IQR Method for Data Cleaning

Due to vibration, external airflow interference, or instrument errors, some data obtained in the test may deviate significantly from adjacent data. These data are called outliers (Figure 7). Outliers can affect the accuracy of the data analysis results [22]. After obtaining the rotational speeds and temperatures of the gas turbine under the different transitional processes, it is necessary to clean the raw test data using specific methods to remove outliers and supplement the missing values. In this study, the IQR method was used to remove outliers [23].

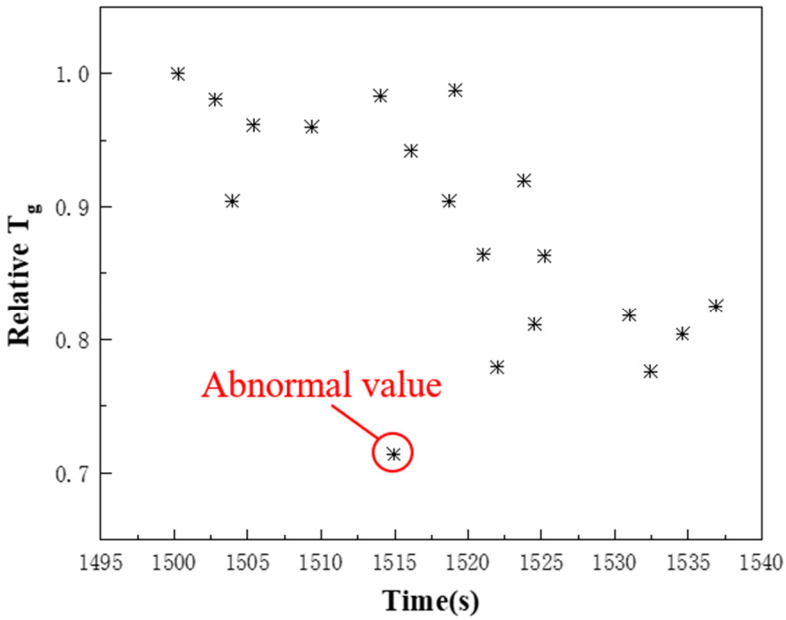

Figure 7. Outliers generated during the testing.

The obtained data were grouped in chronological order. Each group contained 500 data. All values in each group were arranged in ascending order and divided into four equal parts, and the three data located at the points of division were selected as the quartiles of the group. The interquartile range (IQR) is defined as follows, given that, in this sample with all values arranged in ascending order, the 25th percentile value is Q_1, the 50th percentile value is Q_2, and the 75th percentile value is Q_3:

$$IQR = Q_3 - Q_1 \quad (1)$$

The upper and lower limits for this data set were as follows:

$$Q_{min} = Q_1 - 1.5 \times IQR \quad (2)$$

$$Q_{max} = Q_3 + 1.5 \times IQR$$

In this data set, the data beyond the range of [Q_{min}, Q_{max}] were considered outliers and were removed before analyzing the test results. After removing the outliers, we supplemented the original positions of the outliers with averages of the adjacent data points before and after the outlier's original positions.

3.2. Methods for Quantifying the Response Speeds of Controlled Parameters

The primary parameter controlling the transition of the gas turbine from one steady-state operating condition to another is the flow rate of fuel (G_f), called the control parameter. Other parameters are called controlled parameters (e.g., the outlet temperature of the power turbine (T_g), the rotational speed of the high-pressure turbine (N_h), etc.) that change with the flow rate of fuel, but with a certain delay [24]. In this study, the time duration from the end of the change in the control parameter to the end of the change in a controlled parameter was treated as the primary indicator measuring the response speed of the controlled parameter. As shown in Figure 8, during the transition of the gas turbine from steady-state operating condition 1 to steady-state operating condition 2, the time difference Δt_1 between the time t_1 when the fuel flow rate began to change and the time t_2 when the fuel flow rate stabilized is defined as the change time of the fuel flow rate; the time difference Δt_2 between the time t_2 when the fuel flow rate stabilized and the time t_3 when a controlled parameter also reached stability is defined as the response lag time of this parameter; $\Delta t_2/\Delta t_1$ denotes the response lag rate of this controlled parameter. A

longer response lag time and a higher response lag rate indicate a slower response speed of this controlled parameter. When $\Delta t_2 = 0$, it signifies that this controlled parameter responded instantaneously.

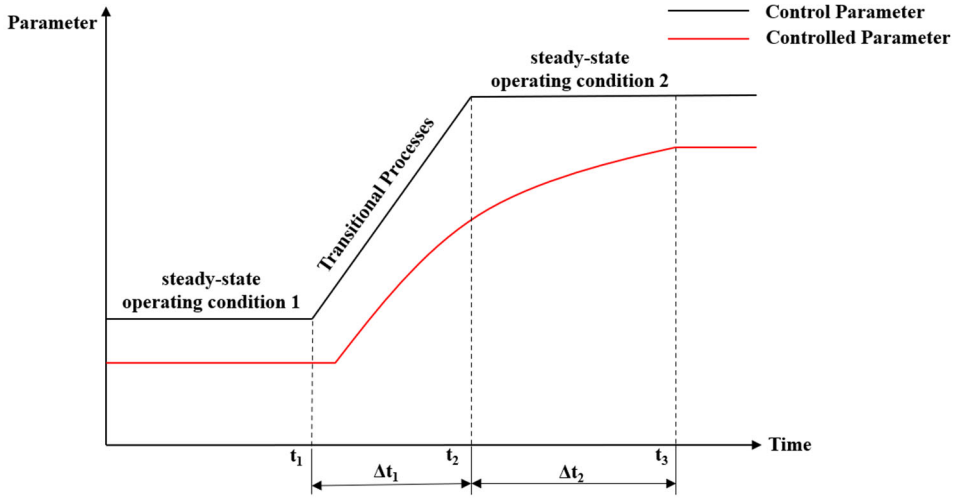

Figure 8. Schematic diagram of variations in control parameters and controlled parameters.

3.3. Methods for Judging the Start and End Times of Parameter Changes

To study the response lag times of the parameters, unified criteria should be established for the time t_1 when the control parameter (i.e., the fuel flow rate G_f) began to change, the time t_2 when Gf reached stability, and the time t_3 when the controlled parameters (T_g and N_h) stabilized. During acceleration: when G_f began rising at a wave trough t and the average value over the subsequent 120 s from t was lower than 120% of the value at t, t was considered as the time t_1 when G_f began to change; when G_f began falling at a wave crest t and the average value over the subsequent 120 s from t was within 80% to 120% of the value at the crest t, t was treated as the time t_2 when G_f reached stability; and when a controlled parameter started reducing at a wave crest t and the average value over the subsequent 120 s from t was within 80% to 120% of the value at the crest t, t was deemed as the time t_3 when this controlled parameter became stable.

For the deceleration process, the value of each parameter near the time of stable operating was small. At this time, the fluctuation ranges caused by such factors as the vibration of the gas turbine and errors in the fuel control system were larger compared to these parameter values. Therefore, the measurement standard for this process was presented by a fixed numerical range instead of percentages. Additionally, the time range for determining the stability was also reduced because of the short deceleration time. During deceleration: when G_f began declining at a wave crest t and the average value over the subsequent 60 s from t was more than 0.1 L/s lower than the value at t, t was considered as the time t_1 when Gf began to change; when G_f began increasing at a wave trough t and the average value over the subsequent 60s from t was within the range of $\pm$0.1 L/s of the value at t, t was regarded as the time t_2 when G_f became stable; and when a controlled parameter started heightening at a wave trough t and the average value over the subsequent 60s from t was within the range of $\pm$50 °C or $\pm$1000 r/min of the value at t, t was deemed as the time t_3 when this controlled parameter stabilized.

4. Test Results and Analysis

In the subsequent text, the relative values of the rotational speed of the high-pressure turbine (N_h), the outlet temperature of the power turbine (T_g), and the flow rate of fuel (G_f) will all be standardized. Under rated load conditions, each parameter is set to a value of 1.

4.1. Axial Temperature Change of the Gas in the Channel

Through the temperature sensors at the three measurement sections z1~z3 of the power turbine outlet, we obtained the axial temperature change law of the gas in this segment of the channel (Figure 9). As presented in Figure 9a, the average gas temperatures measured at the measurement sections z1~z3 over the entire time were 479.8 °C, 478.6 °C, and 474.7 °C, respectively. The axial temperatures decreased by 1.1% on average. The temperatures at the three measurement sections experienced generally consistent change trends and followed the distribution pattern of z1 > z2 > z3. This demonstrates that the gas temperature was subjected to axial gradient variations, which essentially accorded with the test results in other cycles. As shown in Figure 9b, the average gas temperatures measured at the measurement sections z1~z3 were 399.1 °C, 398.9 °C, and 397.8 °C, respectively. The average axial temperature decreased by 0.13%. The temperature distribution at the three measurement sections still followed the pattern of z1 > z2 > z3. This indicates that the heat exchange between the gas and the metal wall cannot completely offset the internal energy loss caused by the expansion work of the gas but partially compensate for this loss. So, the axial declining range of the temperature reduced from 1.1% to 0.13%.

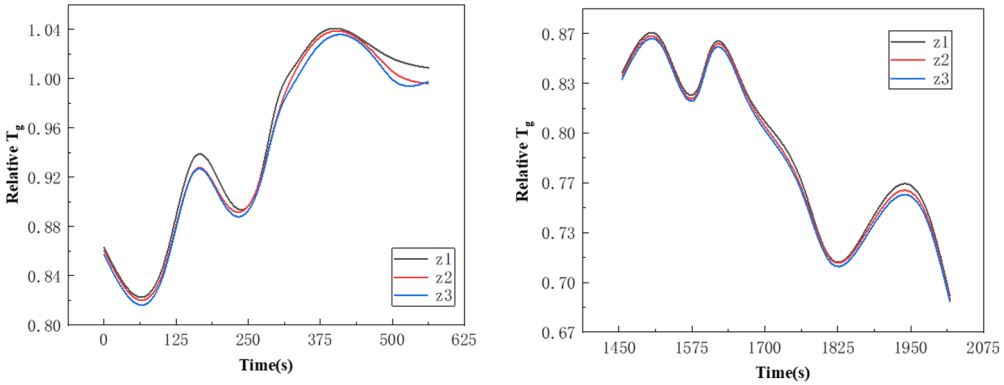

Figure 9. During acceleration (**a**) and deceleration (**b**), gas temperature decreases axially.

4.2. Parameter Change during Cold Start

The data used in this section was acquired from the first cycle of the test when the gas turbine was in a state of cold start. The ambient temperature was 15 °C. After an idle condition of 300 s, the data acquired from the cold start and acceleration to the rated operating condition is shown in Figure 10.

From this cold start to the rated operating condition, t_1 was 300 s, t_2 was 608.25 s, and Δt_1 was 358.25 s. For the controlled parameter T_g, t_3 was 922.25 s, Δt_2 was 314 s, and $\Delta t_2/\Delta t_1$ was 88%. For the controlled parameter N_h, t_3 was 741.25 s, Δt_2 was 133 s, and $\Delta t_2/\Delta t_1$ was 37%. During the cold start condition, the response lag time of the temperature at the outlet of the power turbine was approximately 5.2 min, accounting for 31% of the total time in this transitional stage, with the lag rate reaching 88%. The rotational speed responded faster than the temperature, but still with a response lag of about 2.2 min.

During the cold start, all components of the gas turbine were initially at room temperature. However, the working gas within the channel responded quickly, causing rapid heating in the combustor and channel and creating a large temperature difference with the metal wall. In the initial stage of the start-up, the metal components in contact with the metal wall continuously absorbed heat through thermal conduction, preventing the working gas and the metal wall from reaching a thermal equilibrium quickly. This resulted in a greater impact of thermal inertia on the gas turbine in the cold start state and a longer lag time of temperature response. During the transition from standstill to design rotational speed of the rotor, the gas needed to overcome a large inertia of the rotor. However, there was a loss in total enthalpy when the gas released heat to the metal wall. This weakened the ability of the gas to perform work, prolonging the time to achieve the design rotational

speed. Moreover, the rotor speed did not reach the design value immediately even after stabilizing but only achieved it after the working gas and the wall reached thermal equilibrium and the temperature stabilized for a period. Before the temperature stabilized, the average rotational speed was 2.7% lower than the design value. This loss in rotational speed can be attributed to the loss of total enthalpy during the flow of the gas, which weakened the work capability of the gas.

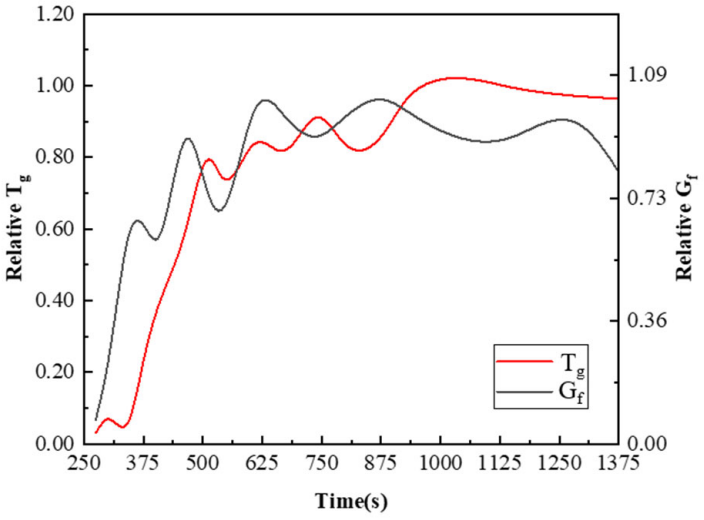

(**a**)

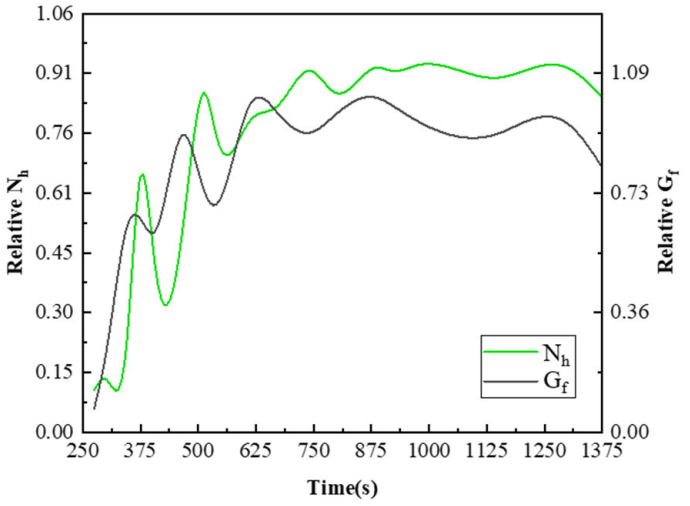

(**b**)

Figure 10. During cold start, changes in G_f, T_g (**a**), and N_h (**b**).

4.3. Parameter Change during Hot Start

In this test, hot start refers to the startup stage in a single cycle ranked in the middle of the 40 operational cycles. Due to the continuous operation, the gas turbine components had been preheated after running for a period. The subsequent tests were conducted in a hot operating state, eliminating the large temperature difference between the metal wall and the gas, as well as the overlong time taking to reach thermal equilibrium as observed during the cold start. Since the results in each cycle under hot operating conditions were generally similar, we only took the data of a cycle ranked in the middle of the operational cycles as an example. Over an idle condition of 300 s, the data during the hot start and acceleration to the rated operating condition are presented in Figure 11.

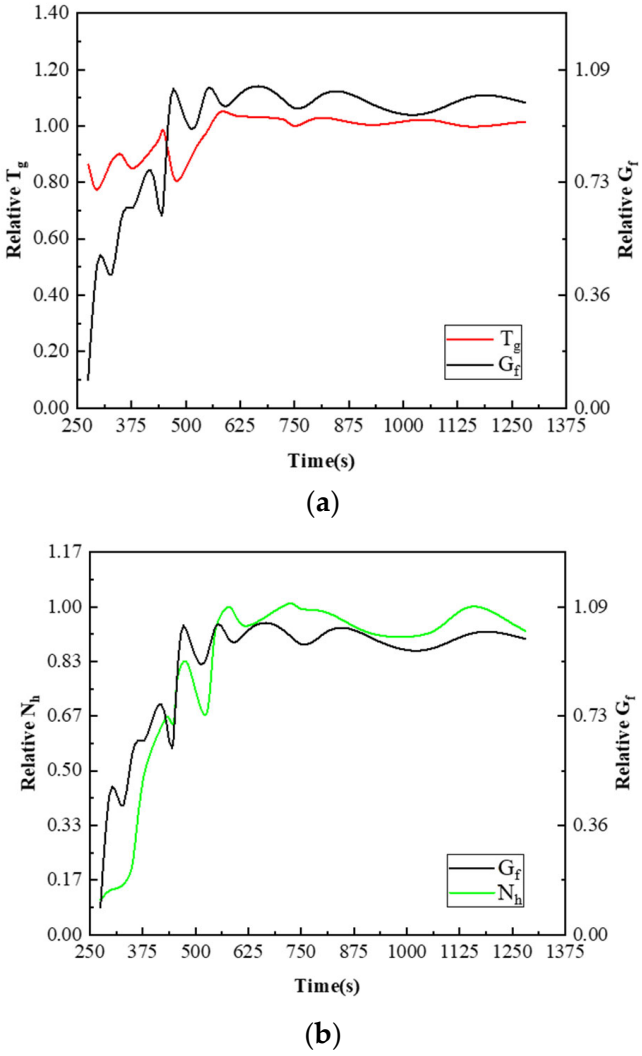

Figure 11. During hot start, changes in G_f, T_g (**a**), and N_h (**b**).

From this hot start to the rated operating condition, t_1 was 300 s, t_2 was 597.5 s, and Δt_1 was 297.5 s. For the controlled parameter T_g, t_3 was 646.5 s, Δt_2 was 49 s, and $\Delta t_2/\Delta t_1$ was 16%. For the controlled parameter N_h, t_3 was 62.25 s, Δt_2 was 31.75 s, and $\Delta t_2/\Delta t_1$ was 11%. During the hot start and acceleration to the rated operating condition, the response lag time of temperature at the outlet of the power turbine reached 49 s; the rotational speed still responded faster than the temperature. However, the difference between the response lag times of the two was as small as less than 5%. In the horizontal comparison, the response lag time of the temperature in this hot start was only 16% of that in the cold start, while the response lag time of the rotational speed was 24% of that observed in the cold start. In addition, T_g fluctuated less throughout the transitional process although it still showed a gradual increase.

During the hot start, the metal wall and other metal components had undergone sufficient preheating, leading to a smaller temperature difference between the gas and the metal wall. Consequently, the time required to reach thermal equilibrium was shorter, and the impact of thermal inertia was reduced during the hot start. In the meantime, the gas had a small loss in total enthalpy so the loss in its mechanical work capability was also small. For this reason, the gas counteracted the rotor inertia and reached the design value more quickly. The rotational speed and temperature stabilized almost simultaneously, and there was no significant drop in the rotational speed during the stabilization. The

stabilized rotational speed was only 0.15% lower than the design value on average. Hence, the rotational speed loss can be negligible.

4.4. Parameter Change during Acceleration

In this test, the acceleration process refers to the stage within each cycle where the gas turbine was accelerated from the 0.2 times rated operating condition to the rated operating condition under the control of the control console. After operating through the previous stages, metal components inside the gas turbine had been preheated to a certain degree. Hence, the gas turbine was in a hot operating condition in the acceleration process. The data of this stage in the first cycle was not greatly different from that in other cycles. Thus, we selected the data of a cycle ranked in the middle of the operational cycles as an example. The data of the gas turbine accelerated are presented in Figure 12.

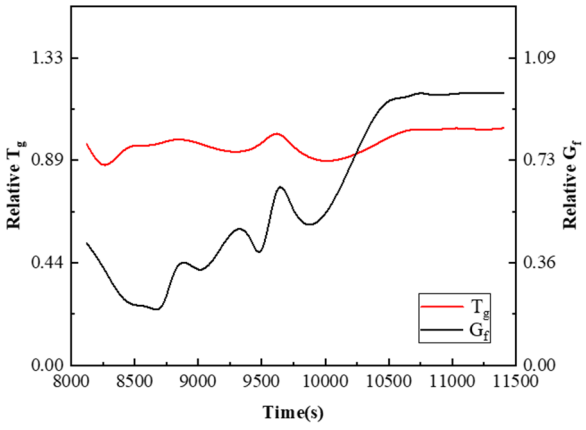

(**a**)

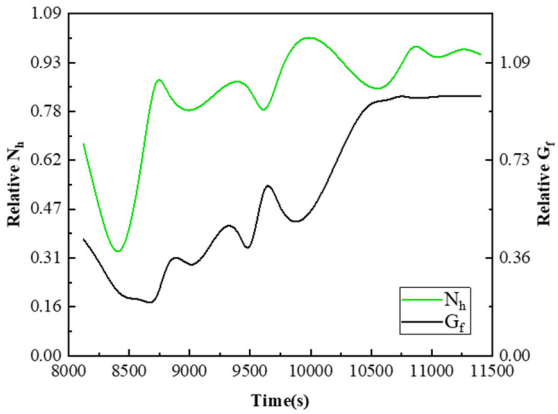

(**b**)

Figure 12. During acceleration, changes in G_f, T_g (**a**), and N_h (**b**).

During this acceleration from the 0.2 times rated operating condition to the rated operating condition, t_1 was 2214 s, t_2 was 2623s, and Δt_1 was 409 s. For the controlled parameter T_g, t_3 was 2657.75 s, Δt_2 was 34.75 s, and $\Delta t_2/\Delta t_1$ was 9%. For the controlled parameter Ng, t_3 was 2707 s, Δt_2 was 84 s, and $\Delta t_2/\Delta t_1$ was 21%. During this acceleration, this was the first time that the rotational speed responded slower than the temperature. The response lag time of the rotational speed was 11% longer than that of the temperature. In a horizontal comparison with the hot start process, T_g in the acceleration process also exhibited an upward trend with a smooth curve on the whole. However, its fluctuation range and increase range were smaller than those in the hot start process. The response lag rate of T_g was 9%, which was lower than that observed in the hot start process, 16%. Yet, the response lag time of the rotational speed was longer than that in the hot start process.

During acceleration, the working condition changed less than in the startup process, so the fuel flow rate from the fuel control system was much (nearly 17% to the maximum) lower than that in the startup process. This difference might lead to a weakening of the temperature increase. Since the gas turbine had been preheated during the acceleration, and the hot start process followed after a shutdown and cooling stage from the previous cycle, the initial temperature of the acceleration process was slightly higher than that of the hot start process and the temperature difference between the gas and the wall was small. Hence, the thermal equilibrium was reached more quickly than in the hot start process, even though the fuel flow rate was low. However, the response lag time of the rotational speed was extended due to the low total enthalpy of the gas, which resulted in a reduced mechanical work capability of the gas to overcome rotor inertia. At this time, only a small heat exchange existed between the gas and the metal wall, and the total enthalpy of the gas experienced little loss, hence almost no loss in the rotational speed. As observed, the rotational speed did not decline sharply in the stabilization process, and the average rotational speed post-stabilization was merely 0.08% lower than the design value.

4.5. Parameter Change during Deceleration

The deceleration process in this test refers to a stage in each cycle where the gas turbine was controlled by the control console to decelerate from the rated operating condition to the 0.2 times rated operating condition. This deceleration process was also a hot-state operating process. As the data of this stage in the first cycle have no large difference from that in other cycles, the data of a cycle ranked in the middle of the operational cycles were taken as an example (Figure 13).

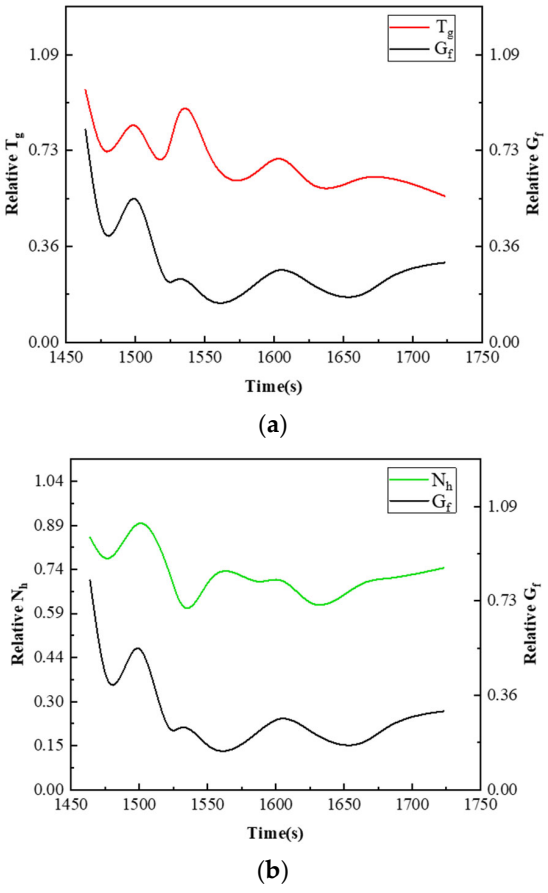

Figure 13. During deceleration, changes in G_f, T_g (**a**), and N_h (**b**).

During this deceleration, t_1 was 1464 s, t_2 was 1523.5 s, and Δt_1 was 59.5 s. For the controlled parameter T_g, t_3 was 1574 s, Δt_2 was 50.5 s, and $\Delta t_2/\Delta t_1$ was 85%. For

the controlled parameter N_h, t_3 was 1527 s, Δt_2 was 3.5 s, and $\Delta t_2/\Delta t_1$ was 6%. In this deceleration process, the temperature response lag time was just second to that in the cold start process. The response lag time of the rotational speed was 3.5 s. Considering errors caused by sensors, the rotational speed was deemed as responding instantaneously during the deceleration. The deceleration process was also influenced by thermal inertia, which might slow down the decrease rates of the controlled parameters. Moreover, the response lags of the rotational speed and temperature were completely different during the deceleration: the temperature response lag time was relatively long, just second to that observed during the cold start, whereas the response lag time of the rotational speed was minimal. A major difference from the acceleration process was that the control parameter G_f changed rapidly, which was related to the fuel control strategy of the gas turbine.

During the deceleration, the fuel control system quickly reduced the fuel flow rate to a low value, and then the gas turbine gradually slowed down by friction on itself. Meanwhile, the temperature of the gas fell; however, the trend was set back because of the metal wall remaining at a high temperature due to the thermal inertia which transferred heat to the gas. Consequently, the temperature response during the deceleration lagged for a longer time. Yet as described in Section 4.1, the heat exchange between the gas and the metal wall cannot completely offset the total enthalpy loss caused by the expansion work of the gas but partially compensate for this loss. Generally speaking, the total enthalpy of the gas declined even if the thermal inertia caused a temperature difference that drove the high-temperature wall to transfer some heat to the gas. Besides, the effect of thermal inertia in delaying the decrease in rotational speed was not significant due to the presence of friction.

5. Conclusions

To investigate the impact of thermal inertia on the dynamic characteristics of a gas turbine under different transitional processes, a test was conducted on a gas turbine test bench. The test lasted for 40 continuous cycles. Each cycle took one hour and included the start-up, shutdown, acceleration, and deceleration processes. Over an analysis of the flow rate of fuel (G_f), the outlet temperature of the power turbine (T_g), and the rotational speed of the high-pressure turbine (N_h), we obtained the following conclusions regarding the impact of thermal inertia on the dynamic characteristics of the gas turbine:

(1) During the transition processes, the gas temperature exhibited an axial gradient distribution in the channel. In both the acceleration and deceleration processes, the gas temperature gradually decreased along the flow direction, just with a slightly great decrease during acceleration and a slightly small decrease during deceleration. This is generally consistent with the results of existing simulation studies.

(2) Thermal inertia posed different extents of impact on the dynamic characteristics of the gas turbine under different transitional processes. During the cold start, the impact of thermal inertia was the most remarkable: the temperature response lag rate reached 88% and the temperature response lag time accounted for 31% of the duration of the whole transitional stage; the response lag time of the rotational speed also reached about 2.2 min. During the hot start and hot-state acceleration, the impact of thermal inertia was small, especially in the hot-state acceleration process. The rotational speed loss caused by thermal inertia was significant only in the cold start process, with the average rotational speed reduced by 2.7% of the design value. The rotational speed losses in other processes were small. Relative to the literature [10], where the temperature response lag rate of the acceleration process averages 8% to 15%, the cold start process far exceeds this simulation value. However, the hot start process is more in line with the simulation results.

(3) In the same transition process, the impacts of thermal inertia on the response speeds of temperature and rotational speed varied. In most transition processes, the response of rotational speed was generally faster than that of temperature. However, during the hot-state acceleration, the response lag time of the rotational speed exceeded that of the temperature. This result is in general agreement with the simulation results

of the literature [5]. This discrepancy was likely related to the initial temperature and fuel flow rate of the gas turbine. The high initial temperature on the metal wall allowed the gas to reach thermal equilibrium with the wall quickly, while the fuel flow rate lower than that in the start-up process required a longer time for the rotational speed to reach the target value.

(4) In the deceleration process, the effect of thermal inertia on the temperature response speed was great, with the temperature response lag time second only to that observed during the cold start. However, the impact of thermal inertia on the rotational speed response was not obvious. During deceleration, the rotational speed response can be considered nearly instantaneous. Relative to the literature [10], the temperature response lag rate of the deceleration process is also much higher than the simulation value. The speed response lag rate is also inconsistent with the simulation results. In the literature [10], the speed response lag rate during the deceleration process is about 3% to 5%, not the instantaneous response. The rapid change in fuel flow rate in the deceleration process caused the low-temperature gas to interact with the metal wall which still retained at a high temperature due to thermal inertia, producing a thermal exchange effect. This effect retarded the decrease in the gas temperature. However, the heat exchange between the gas and the metal wall could not fully offset the internal energy loss caused by the expansion work of the gas. Additionally, the presence of friction made the impact of thermal inertia on the rotational speed response less noticeable. However, the simulation did not take into account the variation of friction with fuel flow. This leads to a large gap between simulation and experimental results for the same deceleration process

Currently, only testing methods have been used to analyze the impact of thermal inertia on the dynamic characteristics of gas turbines. The specific mechanisms of thermal inertia within the channel remain unclear. In future work, a fluid simulation model will be developed to study the internal channels under the mentioned transitional conditions and the internal mechanisms by which thermal inertia affects a gas turbine.

Author Contributions: Conceptualization, Y.L. (Yang Liu); Methodology, Y.L. (Yang Liu); Validation, Y.L. (Yongbao Liu); Resources, Y.L. (Yongbao Liu) and X.L.; Data curation, Y.J. and X.L.; Writing—original draft, Y.L. (Yang Liu); Writing—review & editing, Y.L. (Yongbao Liu) and Y.J. All authors have read and agreed to the published version of the manuscript.

Funding: This research received no external funding.

Data Availability Statement: The original contributions presented in the study are included in the article, further inquiries can be directed to the corresponding author.

Conflicts of Interest: The authors declare no conflicts of interest.

Nomenclature

G_f	fuel flow
T_g	power turbine outlet temperature
N_h	high-pressure turbine speed
t_1	moment the fuel flow begins to change
t_2	moment the fuel flow begins to stabilize
t_3	moment the controlled parameters begins to stabilize
Δt_1	change time of the fuel flow rate
Δt_2	response lag time of the controlled parameter
$\Delta t_2/\Delta t_1$	response lag rate

References

1. Jaw, L.L.; Garg, S. *Propulsion Control Technology Development in the United States A Historical Perspective*; NASA Technical Memorandum, NASA/TM-2005-213978; NASA: Washington, DC, USA, 2005.
2. Yang, Y.; Nikolaidis, T.; Jafari, S.; Pilidis, P. Gas turbine engine transient performance and heat transfer effect modelling: A comprehensive review, research challenges, and exploring the future. *Appl. Therm. Eng.* **2023**, *236*, 121523. [CrossRef]

3. Wortmann, G.; Schmitz, O.; Hornung, M. Comparative assessment of transient characteristics of conventional and hybrid gas turbine engine. *CEAS Aeronaut. J.* **2014**, *5*, 209–223. [CrossRef]
4. Hashmi, M.B.; Lemma, T.A.; Ahsan, S.; Rahman, S. Transient Behavior in Variable Geometry Industrial Gas Turbines: A Comprehensive Overview of Pertinent Modeling Techniques. *Entropy* **2021**, *23*, 250. [CrossRef] [PubMed]
5. Li, Z.J.; Li, Y.G.; Korakianitis, T. Gas turbine transient performance simulation with simplified heat soakage model. In Proceedings of the ASME Turbo Expo 2020: Turbomachinery Technical Conference and Exposition, Virtual, 21–25 September 2020; American Society of Mechanical Engineers: New York, NY, USA, 2020; Volume 84140, p. V005T06A005.
6. Xu, N.; Wang, Q.; Liu, Z.; Yang, F. Transient thermal impact research on turbine rotors based on thermoelastic coupling. *J. Harbin Eng. Univ.* **2016**, *37*, 7.
7. Cao, S.; Xie, Y. Study on Three-Dimensional Thermoelastic Contact Stress of Turbine Blade in High-Temperature Stage Considering Manufacturing Variations. *Therm. Turbine* **2011**, *40*, 103–109.
8. Chapman, J.W.; Guo, T.-H.; Kratz, J.L.; Litt, J.S. Integrated Turbine Tip Clearance and Gas Turbine Engine Simulation. In Proceedings of the 52nd AIAA/SAE/ASEE Joint Propulsion Conference, Salt Lake City, UT, USA, 25–27 July 2016; pp. 1–16. [CrossRef]
9. Kratz, J.L.; Chapman, J.W. Active Turbine Tip Clearance Control Trade Space Analysis of an Advanced Geared Turbofan Engine. In Proceedings of the 2018 Joint Propulsion Conference, Cincinnati, OH, USA, 9–11 July 2018. [CrossRef]
10. Yang, C.; Wu, H.; Du, J.; Zhang, H.; Yang, J. Full-engine simulation of micro gas turbine based on time-marching throughflow method. *Appl. Therm. Eng.* **2022**, *217*, 119213. [CrossRef]
11. Shi, Y.; Tu, Q.; Jiang, P.; Zheng, H.; Cai, Y. Investigation of the compressibility effects on engine transient performance. In Proceedings of the ASME Turbo Expo 2015: Turbine Technical Conference and Exposition, Montreal, QC, Canada, 15–19 June 2015; American Society of Mechanical Engineers: New York, NY, USA, 2015; Volume 56628, p. V001T01A017.
12. Chen, F.; Chen, Y.; Song, K.; Li, Y. Study on the Influence of Heat Transfer Effect on Performance Simulation of Engine Transition State. In Proceedings of the 2019 IEEE 10th International Conference on Mechanical, Brussels, Belgium, 22–25 July 2019.
13. Roclawski, H.; Gugau, M.; Böhle, M. Computational Fluid Dynamics Analysis of a Radial Turbine During Load Step Operation of an Automotive Turbocharger. *J. Fluids Eng.* **2018**, *140*, 1–9. [CrossRef]
14. Visser, W.P.J.; Dountchev, I.D. Modeling thermal effects on performance of small gas turbines. In Proceedings of the ASME Turbo Expo 2015: Turbine Technical Conference and Exposition, Montreal, QC, Canada, 15–19 June 2015; American Society of Mechanical Engineers: New York, NY, USA, 2015; Volume 56628, p. V001T01A014.
15. Visser, W.P.J.; Broomhead, M.J. *GSP A Generic Object-Oriented Gas Turbine Simulation Environment*; NLR: Amsterdam, The Netherlands, 2000.
16. Kiss, A.; Spakovszky, Z. Effects of transient heat transfer on compressor stability. In Proceedings of the ASME Turbo Expo 2018: Turbomachinery Technical Conference and Exposition, Oslo, Norway, 11–15 June 2018.
17. Beard, P.; Adams, M.G.; Nagawakar, J.R.; Stokes, M.; Wallin, F.; Cardwell, D.; Povey, T.; Chana, K. The LEMCOTEC 1.5 Stage Film-Cooled HP Turbine: Design, Integration and Testing in the Oxford Turbine Research Facility. In Proceedings of the 13th European Conference on Turbomachinery Fluid Dynamics & Thermodynamics ETC13, Lausanne, Switzerland, 8–12 April 2019; ETC2019-216.
18. Dong, P.; Amano, R.S. High-pressure gas turbine vane turbulent flows and heat transfer predicted by RANS/LES/DES. In Proceedings of the ASME Turbo Expo 2017: Turbomachinery Technical Conference and Exposition, Charlotte, NC, USA, 26–30 June 2017.
19. Kiss, A. *Two Investigations of Compressor Stability: Spike Stall Inception and Transient Heat Transfer Effects*; Massachusetts Institute of Technology: Cambridge, MA, USA, 2015.
20. Unnikrishnan, U.; Yang, V. A review of cooling technologies for high temperature rotating components in gas turbine. *Propuls. Power Res.* **2022**, *11*, 293–310. [CrossRef]
21. Kumar, R.; Chaterjee, S.; Ranjan, V.; Ghoshal, S.K. Simulation studies on combined effect of variable geometry, rotation and temperature gradient on critical speed of gas turbine disc. *Multidiscip. Model. Mater. Struct.* **2023**, *19*, 277–291. [CrossRef]
22. Boukerche, A.; Zheng, L.; Alfandi, O. Outlier detection: Methods, models, and classification. *ACM Comput. Surv. (CSUR)* **2020**, *53*, 1–37. [CrossRef]
23. Vinutha, H.P.; Poornima, B.; Sagar, B.M. Detection of outliers using interquartile range technique from intrusion dataset. In *Information and Decision Sciences: Proceedings of the 6th International Conference on Ficta, Bhubaneswar, Odisha, 1 January 2018*; Springer: Singapore, 2018; pp. 511–518.
24. Roa, M. Abs rules for integrated power systems (IPS). In Proceedings of the 2009 IEEE Electric Ship Technologies Symposium, Baltimore, MD, USA, 20–22 April 2009; pp. 1–17. [CrossRef]